

# Human Wild-Type Tau Interacts with *wingless* Pathway Components and Produces Neurofibrillary Pathology in *Drosophila*

George R. Jackson,<sup>1</sup> Martina Wiedau-Pazos,  
Tzu-Kang Sang, Naveed Wagle,  
Carlos A. Brown, Sasan Massachi,  
and Daniel H. Geschwind  
Neurogenetics Program  
Department of Neurology  
University of California-Los Angeles  
School of Medicine  
710 Westwood Plaza  
Los Angeles, California 90095

## Summary

Pathologic alterations in the microtubule-associated protein tau have been implicated in a number of neurodegenerative disorders, including Alzheimer's disease (AD), progressive supranuclear palsy (PSP), and frontotemporal dementia (FTD). Here, we show that tau overexpression, in combination with phosphorylation by the *Drosophila* glycogen synthase kinase-3 (GSK-3) homolog and *wingless* pathway component (Shaggy), exacerbated neurodegeneration induced by tau overexpression alone, leading to neurofibrillary pathology in the fly. Furthermore, manipulation of other *wingless* signaling molecules downstream from *shaggy* demonstrated that components of the Wnt signaling pathway modulate neurodegeneration induced by tau pathology in vivo but suggested that tau phosphorylation by GSK-3 $\beta$  differs from canonical Wnt effects on  $\beta$ -catenin stability and TCF activity. The genetic system we have established provides a powerful reagent for identification of novel modifiers of tau-induced neurodegeneration that may serve as future therapeutic targets.

## Introduction

The identification of disease-causing mutations in the microtubule-associated protein tau in some cases of inherited frontotemporal dementia (FTDP-17) demonstrates conclusively that tau abnormalities can cause neurodegeneration (Hutton et al., 1998; Clark et al., 1998; Goedert et al., 1998, 2000). Although tau mutations are identified in only about 10% of inherited FTD cases, a variety of filamentous and nonfilamentous inclusions containing tau are identified in many FTD cases, and hyperphosphorylated filamentous tau comprises the NFT that are a pathological hallmark of PSP and AD (Houlden et al., 1999; Goedert et al., 1998; Lee et al., 2001). Therefore, understanding the events that modify tau-associated neurodegenerative processes is important to further our understanding of the pathophysiology of these diseases and may have relevance for therapeutics.

Many FTD mutations occur in regulatory elements that alter splicing and, thereby, expression of tau isoforms,

rather than tau coding sequence (Clark et al., 1998; Hutton et al., 1998; Hong et al. 1998). Moreover, exhaustive screening has failed to identify tau mutations in AD or the majority of sporadic or familial cases of FTD (Houlden et al., 1999); consequently, tau dysregulation by unidentified *cis*-acting regulatory mutations or other tau-interacting proteins may contribute to tauopathy when it is observed in these conditions. Therefore, we created a *Drosophila* model of tau-related neurodegeneration that does not rely exclusively on mutant tau, but rather on perturbation of wild-type tau expression.

This model provided us with a sensitized genetic system that allowed us to investigate the role of several members of the Wnt signaling pathway, including glycogen synthase kinase-3 $\beta$  (GSK-3 $\beta$ ), in tau-induced neurodegeneration. Components of this pathway, including  $\beta$ -catenin and GSK-3 $\beta$ , have been shown to interact with other proteins implicated in AD, such as presenilin (Killick et al., 2001; Kirschenbaum et al., 2001; Mudher et al., 2001; Palacino et al., 2001). In addition, GSK-3 $\beta$  is a major effector of tau phosphorylation in vitro (Hanger et al., 1992; Lovestone et al., 1994) and in vivo (Lucas et al., 2001). NFT and other pathological forms of tau aggregates are composed of filamentous tau that is hyperphosphorylated on specific serine and threonine residues; however, it is unknown whether tau hyperphosphorylation is causal or secondary to NFT formation in vivo. By manipulation of GSK-3 $\beta$  expression, we were able to demonstrate enhanced neurodegeneration and NFT-like pathology caused by tau hyperphosphorylation in the fly eye. These experiments also support a distinct role for the downstream Wnt signaling components  $\beta$ -catenin and TCF in modulating tau-induced neurodegeneration.

## Results

### Neurodegeneration Induced by Wild-Type Human Tau

The cDNA encoding the longest four repeat isoform of human tau (htau4R) was subcloned into a modified GMR expression vector (Hay et al., 1994; Ollmann et al., 2000), and transgenic *Drosophila* lines were generated. Htau4R transgenic lines (hereafter referred to as gl-tau) demonstrated an abnormal eye phenotype upon eclosion (i.e., emergence from the pupal case as adults). As compared to wild-type (Figure 1A), the gl-tau eyes were reduced in size and displayed a rough phenotype in anterior regions, while posterior aspects appeared normal (Figure 1B). Analysis using scanning electron microscopy (SEM) revealed fused and disordered ommatidia with missing, irregular, and occasional supernumerary mechanosensory bristles. Flies expressing two copies of the transgene had severely reduced eyes (Figure 1C).

In order to determine at what stage the onset of the abnormal phenotype occurs, the larval eye imaginal disc (the primordium of the adult eye) was examined using immunohistochemical staining for the neuronal nuclear protein Elav (Robinow and White, 1988). In third instar

<sup>1</sup>Correspondence: grjackson@mednet.ucla.edu

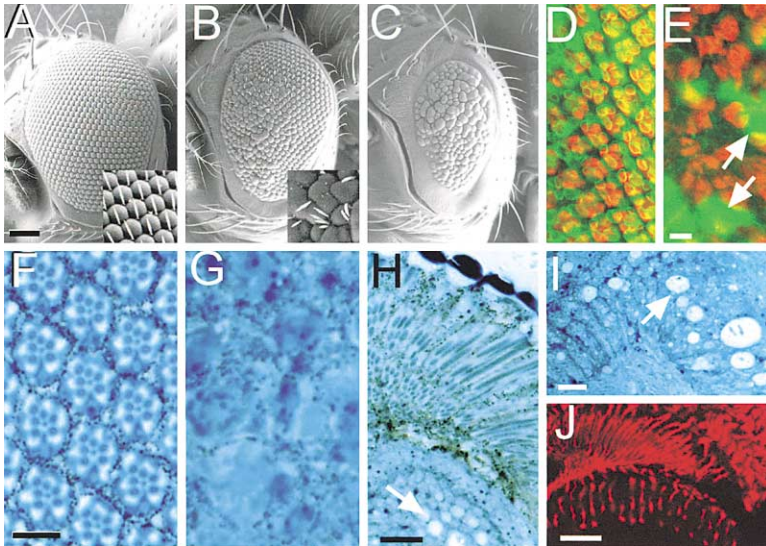


**Figure 1. Phenotype of gl-tau Transgenic Eyes**

(A–C) SEM images of wild-type Berlin (A) and transgenic eyes bearing one ([B] *yw*; *gl-tau-1.1/+*) or two ([C] *yw*; *gl-tau-1.1*) copies of the tau transgene are depicted. Anterior is to the left in (A)–(C). Insets are high-magnification views demonstrating interommatidial bristles. (D and E) Confocal images ([D] control [*yw*] and [E] *yw*; *gl-tau-1.1*) of third instar larval eye imaginal discs are stained with antibodies against the nuclear proteins Elav (red) and lamin (green). The morphogenetic furrow is at the left. Disorganization and cell loss are apparent in the presence of the tau transgenes soon after expression begins ([E]; red: anti-Elav + rhodamine-conjugated anti-rat IgG, green: anti-lamin + FITC-conjugated anti-rabbit IgG). Anterior is to the left in (D) and (E). Arrows, lamin aggregates.

(F and G) Toluidine blue-stained apical tangential sections of wild-type Berlin (F) and two copy tau-overexpressing retinas ([G], *yw*;

*gl-tau-1.1*) show severe tau-induced disorganization of ommatidial architecture with loss of photoreceptor neurons.

(H and I) Longitudinal sections of flies expressing one copy of the tau transgene show severe vacuolization of the medulla (*yw*; *gl-tau-1.1/+*). Arrows, vacuoles.

(J) Confocal image of longitudinal cryostat section shows tau immunoreactivity in the retina and brain. Photoreceptor axons in the lamina and medulla show robust staining using the human tau monoclonal antibody T14 (*cn, bw*; *gl-tau-2.1/+*).

Scale bars: (A–C), 100  $\mu\text{m}$ ; (D and E), 2  $\mu\text{m}$ ; (F and G), 10  $\mu\text{m}$ ; and (H–J), 20  $\mu\text{m}$ .

larval eye discs expressing two copies of the tau transgene, early cell loss, and irregularities in differentiating neurons were apparent soon after tau transgene expression commenced (Figure 1E), compared with the control shown in Figure 1D. Staining using an antibody directed against lamin Dm<sub>0</sub> (a homolog of lamin B) (Smith et al., 1987) demonstrated abnormal accumulation of lamin, which is indicative of nuclear envelope breakdown (Figure 1E), a caspase-mediated process occurring in apoptotic nuclei (Oberhammer et al., 1994; Lazebnik et al., 1995; McCall and Steller, 1998). Loss of photoreceptor neurons and disorganization of the normal (Figure 1F) ommatidial architecture is observed in flies expressing two copies of the tau transgene (Figure 1G). Analysis of the underlying medulla, the second optic ganglion, demonstrated numerous vacuoles (Figures 1H and 1I). Vacuolization has also been observed in a fly model of neurodegeneration due to overexpression of wild-type or the FTD-causing R406W tau mutation, where the appearance of vacuoles was correlated with neurodegeneration (Wittmann et al., 2001). Here, comparison of the pattern of vacuolization with that of tau expression in the medulla was assessed using T14, (Kosik et al., 1988) a monoclonal antibody recognizing an amino terminal epitope of human tau (Figure 1J). Vacuolization was most prominent in the medulla, where tau immunoreactivity was confined to axons of photoreceptors R7 and R8.

#### **GSK-3 $\beta$ /*shaggy* Modulates Tau-Induced Neurodegeneration and NFT-Like Aggregates**

A major source of tau phosphorylation in brain is the serine-threonine kinase, GSK-3 $\beta$ , the human homolog of *Drosophila shaggy/zeste white-3* (Perrimon and Mahowald, 1987). *Shaggy* is a component of the *wingless* signaling pathway (Willert and Nusse, 1998) and serves to phosphorylate Armadillo (the *Drosophila* homolog of

$\beta$ -catenin), thus targeting it for degradation via the ubiquitin-proteasome pathway (Pai et al., 1997). We assessed interactions between tau and the *wingless* pathway, using several transgenes and loss-of-function mutations. Transgenes were expressed using the binary GAL4/UAS system (Brand and Perrimon, 1993), allowing us to target their expression to cell populations overlapping with those expressing tau. In a background heterozygous for a hypomorphic allele of *shaggy*, the tau eye phenotype was ameliorated, producing larger eyes with a more normal ommatidial array except at the most anterior margin of the eye (data not shown). This effect was subtle when the effect of the *shaggy* loss-of-function was assessed in conjunction with one copy of the tau transgene, but was dramatic when the transgene copy number was increased; two copies of *gl-tau* produced a severely reduced eye phenotype (Figure 2A), which was dramatically suppressed in a background heterozygous for a loss-of-function mutation in *shaggy* (Figure 2B). We employed a pan-neural driver that had been exploited previously to examine effects of *shaggy* overexpression in the eye (Ahmed et al., 1998), the *elav-GAL4<sup>C155</sup>* line (Lin and Goodman, 1994). In *trans* to *elav-GAL4*, UAS-*shaggy* had no visible external phenotype other than mildly disordered bristles (data not shown). In the presence of *gl-tau*, however, *shaggy* exerted a dramatic effect. Coexpression of tau throughout the retina, in combination with pan-neural expression of *shaggy*, resulted in a markedly reduced eye with complete loss of normal ommatidia and the majority of bristles (Figure 2D).

We examined the retinal localization of tau coexpressed with *shaggy* using the monoclonal antibody AT100, which recognizes a phosphorylated epitope unique to tau within PHF (Matsuo et al., 1994). AT100 staining is specific for intraneuronal and extraneuronal

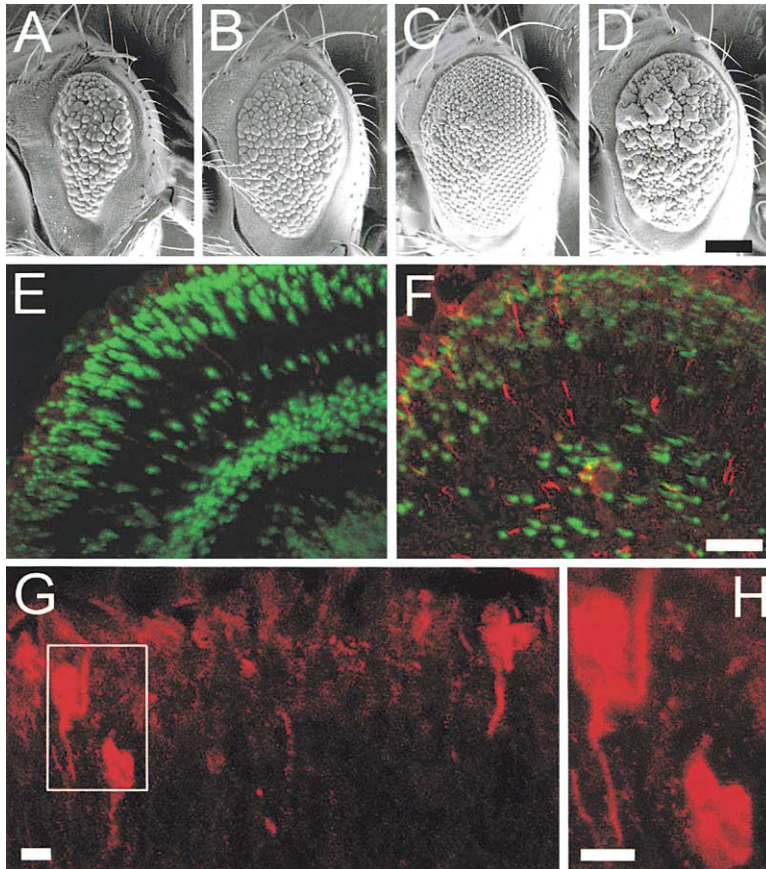


**Figure 2. *shaggy* Loss-of-Function Suppresses, Whereas Pan-Neural Overexpression of *shaggy* Enhances, the Tau Rough Eye Phenotype and Results in the Formation of NFT-Like Fibrillar Inclusions**

(A–D) SEM images of *yw*; *gl-tau-1.1/+*; *gl-tau-2.1/+* (A), *sgg<sup>1/+</sup>*; *gl-tau-1.1/+*; *gl-tau-2.1/+* (B), *yw*; *gl-tau-1.1/+* (C), and *elav-GAL4/+*; *gl-tau-1.1/+*; *UAS-sgg/+* (D) show suppression of the two copy tau phenotype in a background heterozygous for a *shaggy* mutation and enhancement with pan-neural overexpression of *shaggy*. Anterior is to the left in (A–D).

(E–H) Confocal analysis of cryostat sections using an antibody recognizing phosphorylated PHF-tau. (E) (*elav-GAL4/+*; *cn, bw*; *gl-tau-2.1/TM6B*) shows negligible staining of phosphotau in the retina, but (F)–(H) (*elav-GAL4/+*; *cn, bw*; *gl-tau-2.1/UAS-sgg*) show aggregates of phosphorylated tau with pan-neural *shaggy* expression. Red: AT100 + Cy3-conjugated anti-mouse IgG. Green: DAPI. Nuclear disorganization accompanies the more severe neurodegenerative phenotype. (G) Neurofibrillary aggregates show AT100 immunoreactivity in dystrophic neurites and cell bodies. Box, enlargement shown in (H). In (F), the section is more laterally oriented than shown in (G) and (H). Scale bars: (A–D), 100  $\mu$ m; (E and F), 20  $\mu$ m; and (G and H), 10  $\mu$ m.

NFT in AD, recognizing a compound phosphorylated epitope in NFTs, but not tau in its native fetal or adult state or in pretangles (Hoffmann et al., 1997; Zheng-Fischhofer et al., 1998; Augustinack et al., 2002). No staining for AT100 was observed in the wild-type (data not shown), whereas traces of diffuse staining were observed in tau transgenic eyes (Figure 2E). Strikingly, in flies coexpressing *shaggy* and tau within photoreceptor neurons, abundant discrete flame-shaped and fibrillar aggregates were observed throughout the retina and underlying lamina and medulla (Figure 2F). Dystrophic neurites and cell bodies containing hyperphosphorylated tau with morphology reminiscent of NFT were observed with AT100 staining (Figures 2G and 2H).

The appearance of fibrillar phosphotau aggregates with *shaggy* misexpression correlated with increased tau immunoreactivity with AT100 using immunoblots of *gl-tau* heads (Figure 3A). Minimal AT100 tau immunoreactivity was observed in the *gl-tau* flies alone, whereas a more abundant signal was observed with heads coexpressing *gl-tau* and *shaggy*, correlating with the immunohistochemical presence of fibrillar aggregates of tau. Electron microscopy of insoluble extracts was performed to ascertain the conformation of the filamentous tau-containing aggregates. Filament formation was not observed in the wild-type background or in flies expressing *gl-tau* alone. In the presence of both the tau and *shaggy* transgenes, however, filamentous structures, including PHF showing a characteristic periodicity similar

to those extracted from the AD brain, were observed (Figures 3B–3D; Crowther 1991; Crowther et al. 1992). The filament shown in Figure 3B is approximately 410 nm long, 30 nm wide at its thickest point, and has a periodicity of 45 nm; these measurements are within the range of 75 to 550 nm length, 8 to 40 nm width, and 40 to 80 nm periodicity observed in human PHF. Straight filaments (another form of pathological filamentous tau), which are considered a structural variant of PHF (Crowther 1991), were also observed to be within the size ranges observed in AD. Three straight filaments from fly brain shown in Figures 3C and 3D are approximately 160 to 210 nm long and 20 nm wide, and the filament derived from postmortem AD brain extracted concurrently with the fly heads is approximately 290 nm long and 20 nm wide (Figure 3E), consistent with previous measurements in postmortem brain. Thus, phosphorylation of human tau by the *Drosophila* GSK-3 homolog *Shaggy* resulted in the formation of neurofibrillary pathology, including straight filaments and PHF, whereas these structures were not observed in flies overexpressing tau alone.

Given the enhanced rough eye phenotype and appearance of neurofibrillary-like aggregates containing hyperphosphorylated tau in flies coexpressing tau and *shaggy*, we sought to determine the relationship between the appearance of AT100 immunoreactivity and neurodegeneration. In third instar larval eye discs expressing one copy of *gl-tau*, only subtle irregularities

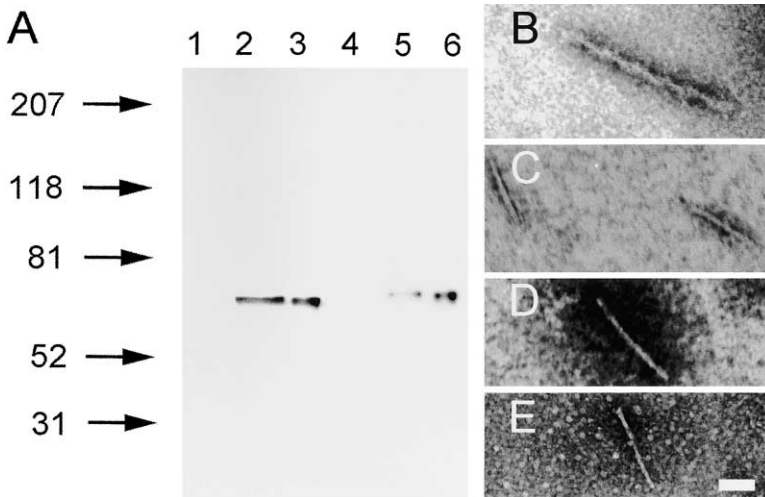


Figure 3. Coexpression of *shaggy* and Tau Produces Increased AT100 Signal on Immunoblots and Abnormal Filaments by Electron Microscopy

(A) Immunoblot, using heads of flies expressing tau either alone (lane 2) or with *shaggy* (lane 3), shows comparable levels of tau as assessed using a phosphorylation-independent antibody (T14). Using a phosphotau antibody (AT100), minimal signal is observed with tau alone (lane 5), but increased signal is seen in the presence of both tau and *shaggy* (lane 6). Quantitation of the AT100 immunoreactivity in two independent pools each of *shaggy* + gl-tau and gl-tau fly heads normalized for T14 signal revealed an increase of more than 2-fold ( $2.07 \pm 0.33$ , mean  $\pm$  SD) in AT100 immunoreactivity in *shaggy* + gl-tau flies, as compared to those expressing tau alone. No signal was observed in the wild-type background with either antibody (lanes 1 and 4). A longer exposure was used for AT100, as

compared to T14, for the figure. Genotypes are as follows: lanes 1 and 4, wild-type Berlin; lanes 2 and 5, *elav-GAL4/+; gl-tau-1.1/+; UAS-sgg/+*; and lanes 3 and 6, *elav-GAL4/+; gl-tau-1.1/+; UAS-sgg/+*. (B–D) Appearance of filaments derived from flies expressing both tau and *shaggy* (*elav-GAL4/+; gl-tau-1.1/+; UAS-sgg/+*) is depicted. The PHF are all shown at the same scale (bar: 200 nm, [E]).

were observed using double staining for lamin and Elav (Figure 4A). In flies coexpressing tau and *shaggy*, however, focal aggregates of AT100-positive signal were surrounded by areas of absent Elav staining with either abnormal or absent lamin staining, indicating ongoing nuclear breakdown and cell death (Figure 4B). However, massive accumulation of lamin, such as that observed with two copies of gl-tau (Figure 1E), was not observed with one copy in combination with *shaggy*. We then examined the appearance of phosphorylated tau and the morphology of the eye disc in a midpupal stage (70%). Tangential views showed mild abnormalities in ommatidial orientation in the presence of gl-tau, but otherwise the eye discs were fairly normal (Figure 4C). Only trace AT100 immunoreactivity was observed. In the presence of both tau and *shaggy*, however, more severely malformed rhabdomeres were observed (Figure 4D). Focal AT100 immunoreactivity was observed along the posterior aspects of the rhabdomeres, where microtubules are known to localize (Fan and Ready, 1997). Lamin staining showed a more intense intranuclear pattern rather than the distinct inner nuclear membrane appearance seen in the absence of *shaggy*, indicating ongoing apoptosis in the pupal stage. Finally, we compared the appearance of the adult retina of gl-tau transgenic eyes in the absence (Figure 4E) and presence (Figure 4F) of overexpressed *shaggy* using toluidine blue-stained tangential sections. In the absence of *shaggy*, minor abnormalities of ommatidial orientation were observed, with occasional missing rhabdomeres and fused ommatidia (Figure 4E). In the presence of *shaggy*, ommatidial architecture was highly irregular, with severely misoriented rhabdomeres. The normal pattern of pigment surrounding each ommatidium (e.g., in Figures 1F and 4E) was lost, with only traces of pigmentation. Vacuolization of the retina was also apparent. Taken together, these findings indicate that tau hyperphosphorylation induces early onset, progressive neu-

rodegeneration. Focal aggregates of AT100 immunoreactivity were apparent soon after tau expression commenced; neurodegeneration was apparent in the larval eye disc but became progressively more severe in pupae and adults.

#### $\beta$ -Catenin/*armadillo* and TCF Modify Tau-Induced Neurodegeneration

Given the success obtained in modifying the tau phenotype via manipulation of *shaggy* expression, the effects of two other *wingless* pathway components downstream of *shaggy* were assessed: *armadillo*, the fly homolog of  $\beta$ -catenin (Riggelman et al., 1989), and *pangolin*/dTCF, the fly homolog of TCF (Brunner et al., 1997). When *wingless* signaling occurs, *Shaggy* activity is inhibited, decreasing *Armadillo* phosphorylation and facilitating its translocation into the nucleus to act as a transcriptional coactivator of dTCF (Willert and Nusse, 1998). If potentiation of the gl-tau rough eye phenotype by *shaggy* overexpression occurred via antagonism of the *wingless* pathway, loss-of-function mutations in *armadillo* would have the opposite effect of those in *shaggy*, since the former would suppress, whereas the latter would activate, *wingless* signaling. Instead, we observed that two mutations in *armadillo* suppressed the tau phenotype, resulting in restoration of the eye to near wild-type size with a more regular external appearance, except at the anterior margin (Figures 5A–5C). In order to assess the effect of *armadillo* gain-of-function, stabilized *arm* (UAS-*arm*.S10; Pai et al., 1997) was expressed under *sevenless* (*sev*)-GAL4 (Brunner et al., 1994) control in order to minimize phenotypic effects in the absence of tau by restricting expression to cone cells and a subset of photoreceptor neurons. The *sev*-GAL4 driver alone has no effect on the gl-tau phenotype (Figure 5D). A slightly different stabilized form of *armadillo* induces death of photoreceptor neurons when expressed under control of *sevenless* (Ahmed et al., 1998). Under *sev*-

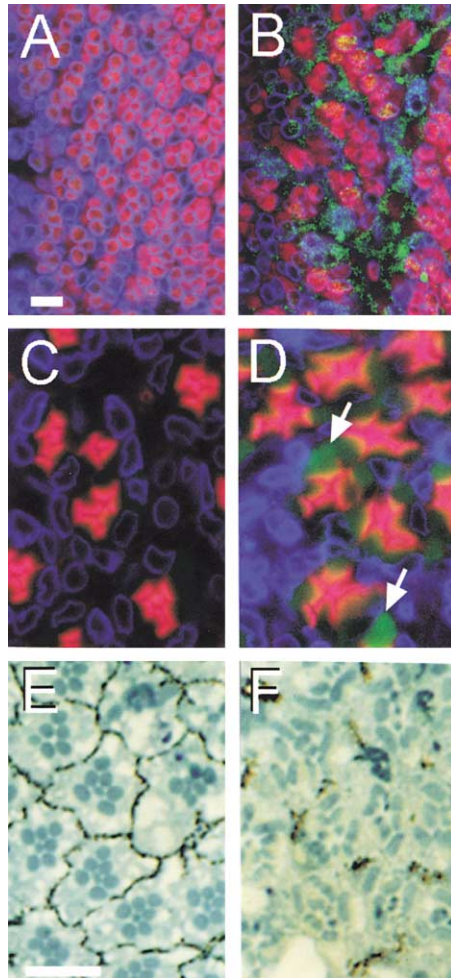


**Figure 4. Overexpression of *shaggy* Results in Early Tau Phosphorylation and Exacerbation of Neurodegeneration**

(A–B) Third instar larval eye discs stained with anti-lamin (blue; Cy5-conjugated anti-rabbit IgG), anti-Elav (red; rhodamine-conjugated anti-rat IgG), and AT100 (green; FITC-conjugated anti-mouse IgG) are depicted. Irregularities of lamin and Elav staining indicating ongoing apoptosis, as well as appearance of discrete phosphotau aggregates, are apparent in discs expressing both tau and *shaggy* ([B], *elav-GAL4/+; gl-tau-1.1/+; UAS-sgg/+*). No AT100 staining is observed in the absence of the *shaggy* transgene, and only minor irregularities in nuclear staining are observed ([A], *elav-GAL4/+; gl-tau-1.1/+; TM6B/+*).

(C and D) Midpupal (70%) eye discs stained with phalloidin-rhodamine (red), lamin (blue; Cy5-conjugated anti-rabbit IgG), and AT100 (green; FITC-conjugated anti-mouse IgG) are shown in (B) and (C). Minor irregularities in ommatidial orientation are observed in the absence of the *shaggy* transgene with only traces of AT100 staining (C), *elav-GAL4/+; gl-tau-1.1/+; TM6B/+*). In the presence of overexpressed *shaggy* (D), more irregularities in the rhabdomere structure are observed with abnormal lamin staining indicating nuclear envelope breakdown. Intense AT100 staining is observed along posterior aspects of rhabdomeres (arrows; *elav-GAL4/+; gl-tau-1.1/+; UAS-sgg/+*).

(E and F) Toluidine blue-stained apical tangential sections of adult retina. In the absence of overexpressed *shaggy* (E), subtle irregularities in ommatidial orientation are observed, with occasional fused ommatidia and missing rhabdomeres (*elav-GAL4/+; gl-tau-1.1/+; TM6B/+*). When *shaggy* is overexpressed (F), ommatidia become highly disorganized, with abnormally oriented rhabdomeres and pigmentation (*elav-GAL4/+; gl-tau-1.1/+; UAS-sgg/+*).

Scale bars: (A and B), 3  $\mu$ m and (C–F), 10  $\mu$ m.

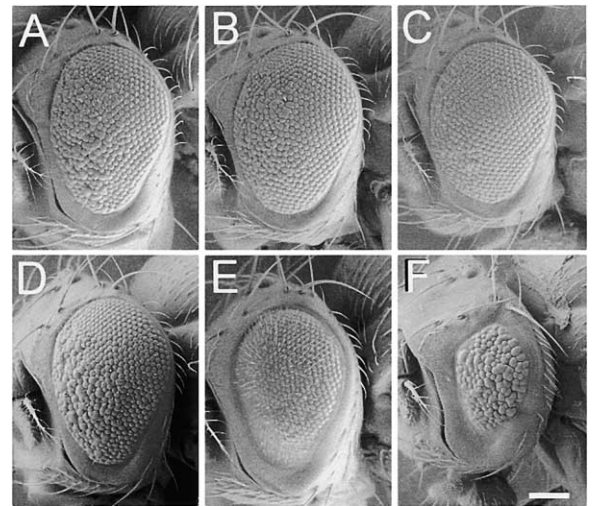


**Figure 5. *armadillo* Loss-of-Function Mutations Suppress, Whereas Misexpression of Stabilized *armadillo* Enhances, the *gl-tau* Phenotype**

(A–C) SEM images of *yw; gl-tau-1.1/+* (A), *arm<sup>1</sup>/+; gl-tau-1.1/+* (B), and *arm<sup>4</sup>/+; gl-tau-1.1/+* (C) show suppression of the tau phenotype in flies heterozygous for two different *armadillo* mutations.

(D–F) Images of *yw/y; gl-tau-1.1/sev-GAL4(S)* (D), *UAS-arm.S10/y; sev-GAL4(S)/+* (E), and *UAS-arm.S10/y; gl-tau-1.1/sev-GAL4(S)* (F) show a mildly reduced eye with disordered bristles with misexpression of stabilized *armadillo* alone, which is enhanced by coexpression with tau, yielding a severely reduced eye with complete loss of normal ommatidia and bristles.

Scale bar: 100  $\mu$ m.

*enless* control, *arm.S10* expression resulted in a mildly reduced eye with disordered bristles (Figure 5E). The *gl-tau* and stabilized *armadillo* transgenes showed a synergistic effect, producing markedly reduced eyes with complete loss of ommatidial borders and bristles (Figure 5F). Thus, perturbation of *armadillo* expression showed effects opposite those expected if the pathological effects of *shaggy* occurred via Armadillo phosphorylation and its subsequent downregulation, rather than via an independent, direct effect of *shaggy* on tau phosphorylation.

We next evaluated the effects of altering dTCF expression on the tau-induced phenotype. A loss-of-function mutation in dTCF resulted in subtle amelioration of the phenotype, with the rough aspect apparent only in more anterior portions of the eye (Figures 6A and 6B). Overexpression of dTCF using both the *elav*- and *sev-GAL4* drivers was lethal, so a weaker version of the *sev-GAL4* driver (Therrien, et al., 1999) was used. Under control of this *sev-GAL4* driver, UAS-dTCF showed a normal external phenotype other than subtle bristle abnormalities (data not shown). In the presence of both the tau and dTCF transgenes, an enhanced rough appearance to the anterior aspect of the eye was apparent, with fusion, pitting, and collapse of ommatidia, as well as loss and irregularities of bristles (Figures 6C and 6D). Thus, manipulation of dTCF and *armadillo* showed comparable effects, with loss-of-function mutations suppressing and overexpression enhancing the tau phenotype.

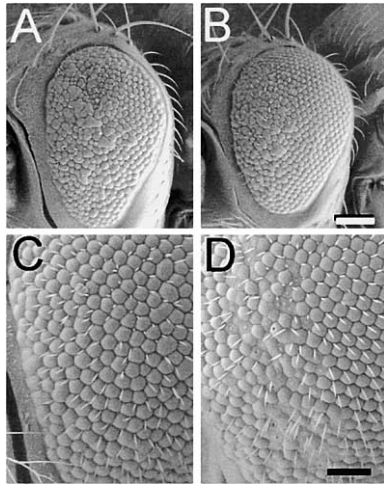


**Figure 6. dTCF Loss-of-Function Mutation Suppresses, Whereas Misexpression of dTCF Enhances, the *gl*-tau Phenotype**  
(A and B) SEM images of *yw*; *gl*-tau-1.1/+ (A) and +; *gl*-tau-1.1/+; +; dTCF<sup>2/+</sup> (B) show that the tau phenotype is mildly suppressed in eyes heterozygous for a null dTCF mutation.  
(C and D) Images of *w*; *sev*-GAL4 (W)/+; *gl*-tau-2.1/+ (C) and *w*; *sev*-GAL4 (W)/UAS-dTCF; *gl*-tau-2.1/+ (D) show enhancement of the tau eye phenotype at the anterior margin of the eye in flies overexpressing dTCF. Overexpression of dTCF alone (data not shown) yields essentially normal eyes with subtle bristle abnormalities (*w*; *sev*-GAL4 (W)/UAS-dTCF).  
Scale bars: (A and B), 100  $\mu$ m and (C and D), 50  $\mu$ m.

### Inhibitors of Apoptosis Suppress Tau-Induced Neurodegeneration

The effects of three well-characterized anti-apoptotic genes, DIAP-1, DIAP-2 (Hay et al., 1995), and P35 (Hay et al., 1994), on the tau phenotype were then assessed. Each of the three apoptotic inhibitors tested partially suppressed the *gl*-tau phenotype (Figure 7A), resulting in restoration of the eye toward wild-type size with a less rough external appearance (Figures 7B–7D). The ability of the apoptotic inhibitor transgenes to suppress the tau phenotype was incomplete but comparable to that of the heterozygous *armadillo* mutations. These data, in conjunction with abnormalities observed in the pattern of nuclear lamin staining, strongly support a role for apoptosis in tau-induced neurodegeneration.

### Discussion

Here, human tau was overexpressed in the *Drosophila* eye to create a model of neurodegeneration based on perturbation of wild-type tau expression, as well as to

enable genetic screening for modifiers of tau-associated neurodegeneration. We tested for genetic interactions between tau-induced neurodegeneration and the Wnt pathway using GSK-3 $\beta$  and two additional components,  $\beta$ -catenin/*armadillo* and dTCF, which are downstream of GSK-3 $\beta$ . Overexpression of wild-type htau4R in *Drosophila* resulted in degeneration without apparent accumulation of NFT, as observed in previous models (Williams et al., 2000; Wittmann et al., 2001). However, we observed that tau hyperphosphorylation by the *Drosophila* GSK-3 $\beta$  homolog Shaggy exacerbated tau-induced neurodegeneration, resulting in the formation of NFT-like filamentous tau aggregates, thus showing a causal relationship between tau hyperphosphorylation and neurofibrillary pathology in vivo. These findings suggest that tau phosphorylation by the fly GSK-3 $\beta$  homolog has a direct influence on the aggregation of tau in vivo, which is likely independent of its classical Wnt role (i.e., enhancement of  $\beta$ -catenin degradation). These data further establish the Wnt pathway as a mediator of tau-induced neurodegeneration and demonstrate that factors other than phosphorylation can modulate neurodegeneration associated with tau dysregulation.

### A Distinct Role for the Wnt/*wingless* Pathway

The enhancement of tau-induced neurodegeneration observed in conjunction with GSK-3 $\beta$  misexpression led us to assess the effects of manipulating expression of  $\beta$ -catenin/*armadillo* and TCF, which are downstream of GSK-3 $\beta$  in the canonical Wnt signaling pathway. The Wnt pathway, originally described as the *wingless* pathway in *Drosophila*, is crucial for axis formation and regionalization of the vertebrate body and nervous system (Cadigan and Nusse, 1997; Peifer and Polakis, 2000). The activity of GSK-3 $\beta$  is inhibited as a consequence of Wnt signaling (Cadigan and Nusse, 1997; Dale, 1998). In the absence of the Wnt signal, GSK-3 $\beta$  phosphorylation of  $\beta$ -catenin leads to its degradation and thus impairs the ability of  $\beta$ -catenin to serve as a coactivator of the transcription factor TCF. Therefore, if GSK-3 $\beta$  overexpression were exerting its tau-modifying effect indirectly via enhancement of  $\beta$ -catenin phosphorylation, loss of  $\beta$ -catenin or TCF function would mirror the effect of GSK-3 $\beta$  overexpression. In contrast, increased  $\beta$ -catenin or TCF activity, as it occurs following Wnt binding to its receptor, would be expected to exert an effect opposite to that of GSK-3 $\beta$  overexpression.

This was not observed. Instead, increased expression of either  $\beta$ -catenin/*armadillo* or TCF enhanced the tau-induced neurodegenerative phenotype, whereas loss-of-function mutations in  $\beta$ -catenin/*armadillo* or TCF

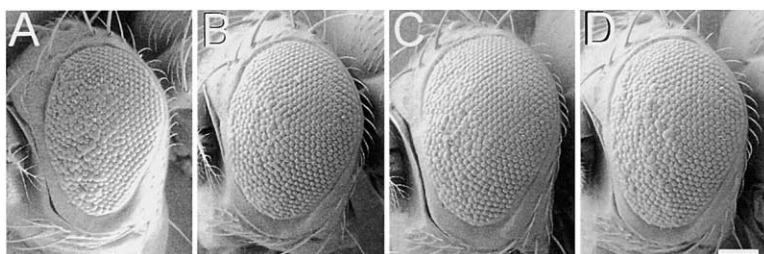


**Figure 7. Inhibitor of Apoptosis Proteins Suppress the *gl*-tau Phenotype**

As compared to flies expressing one copy of the tau transgene alone ([A] *yw*; *gl*-tau-1.1/+), coexpression of DIAP1 ([B] GMR-DIAP-1/+; *gl*-tau-1.1/+), DIAP-2 ([C] *yw*; *gl*-tau-1.1/+; GMR-DIAP2), or P35 ([D] *yw*; *gl*-tau-1.1/+; GMR-P35/+) suppresses the phenotype, restoring eye size toward normal. Scale bar: 100  $\mu$ m.

repressed it. Thus, results of the manipulation of two targets downstream of GSK-3 $\beta$  in the Wnt pathway are most consistent with the notion that when overexpressed in the context of human tau dysregulation, GSK-3 $\beta$ /*shaggy* is not exerting its primary effect in this model via the canonical Wnt pathway but, rather, via direct tau hyperphosphorylation (Godemann et al., 1999; Ishiguro et al., 1993; Mandelkowitz et al., 1992; Mulo et al., 1994). If their effects are indeed independent, as suggested by the current observations, one might also expect  $\beta$ -catenin/*armadillo* and GSK-3 $\beta$ /*shaggy* overexpression or loss-of-function mutations to be additive in the gl-tau background, an outcome that can be assessed in future studies. Further support for these conclusions comes from the observation of a  $\beta$ -catenin-independent, proapoptotic effect of GSK-3 $\beta$  in primary cortical neuronal cultures (Hetman et al., 2000). The predominance of the direct effect of *shaggy* phosphorylation of tau over downstream Wnt pathway signals in the current model may be attributed to a recently identified requirement for  $\beta$ -catenin priming by casein kinase I $\alpha$  phosphorylation prior to its phosphorylation by GSK-3 and subsequent degradation (Liu et al., 2002) It will now be important to examine the effects of *shaggy* overexpression on Armadillo phosphorylation and stability more closely, with attention to a potential role for casein kinase I $\alpha$  priming in the gl-tau model.

Previous work has shown a role for the Wnt pathway and, specifically,  $\beta$ -catenin in apoptosis in the nervous system in *Drosophila* (Ahmed et al., 1998; Freeman and Bienz, 2001) and the mouse (Hasegawa et al., 2002). Therefore, the modulatory effects of  $\beta$ -catenin and TCF on the neurodegeneration observed here suggested a function for apoptotic cell death in degeneration associated with gl-tau. The role of apoptosis in tau-induced neurodegeneration was confirmed by changes in lamin staining, indicating breakdown of the nuclear envelope, which is a typical feature of apoptosis in *Drosophila* and mammalian systems (Oberhammer et al., 1994; Lazebnik et al., 1995; McCall and Steller, 1998). This was further demonstrated by amelioration of tau-induced cell death by overexpression of three anti-apoptotic genes. Recent work demonstrates a role for GSK-3 $\beta$  phosphorylation of tau in neuronal apoptosis in rat brain (Elyaman et al., 2002). Apoptosis has also been implicated in neurodegeneration in cell lines expressing tau harboring several different FTDP-17-causing mutations (Furukawa et al., 2000), in a mouse model of FTDP-17-expressing mutant tau (Gotz et al., 2001), and in autopsy tissue from FTD patients (Su et al., 2000). These studies support the relevance of the current findings in *Drosophila* to FTD in humans and other models of tauopathy. Not all cases of FTD involve tau (Morris et al., 2001; Lee et al. 2001), so whether apoptosis is a major mechanism of neuronal death in non-tau-related FTD awaits further investigation.

#### The Effect of Tau Misexpression on Neural Development and Cell Fate

Examination of the effects of moderate tau overexpression suggests that the gl-tau phenotype is due to significant alterations in cell fate decisions, as well as progressive neurodegeneration. As many as four interommatidial bristles were observed in eyes expressing

one copy of gl-tau (Figure 1B, inset). We surmise that these developmental effects may also be due to interactions with Wnt signaling. In the *Drosophila* eye, ectopic *wingless* expression suppresses interommatidial bristle formation by repressing *achaete* expression, using a pathway requiring *armadillo* (Cadigan and Nusse, 1997). Sensory organ precursors in the pupal eye disc are selected to form interommatidial bristles. Eye-specific overexpression of the intracellular domain of E-cadherin, which attracts Armadillo to adherens junctions and thus inhibits its signaling function (Sansom et al., 1996), also generates supernumerary bristles (Greaves et al., 1999). The increase in severity of neurodegeneration observed in the current model of tau overexpression follows an anterior-posterior gradient that parallels the pattern of *wingless* expression in the larval eye disc (Ma and Moses, 1995), again consistent with the modulatory effects of Wnt signaling observed here. These developmental interactions between pathological tau expression and the Wnt pathway, a critical player in CNS regionalization, are also supportive of the idea that developmental perturbations may underlie the regional vulnerability observed in focal neurodegenerative syndromes, such as FTD (Geschwind and Miller, 2001; Geschwind et al. 2001).

#### The Role of Phosphorylation in Fibrillar Tau Aggregation

A large body of literature demonstrates that tau present in many forms of insoluble pathological aggregates, including NFT in AD and FTD, is abnormally phosphorylated on specific serine and threonine residues detected by AT100 and other antibodies (Goedert et al., 1998; Lee et al., 2001). Among these antibodies, the AT100 epitope defines NFT-tau most unambiguously, since it does not react with tau in the normal brain or tau that is in a pretangle, nonfilamentous conformation (Zheng-Fischhofer et al. 1998; Augustinack et al., 2002). Thus, the presence of the AT100 epitope that has been shown to be specific for tau in the intracellular and extracellular tangle stage in AD (Augustinack et al., 2002) strongly supports the presence of NFT-like inclusions in this fly model. EM studies further strengthen this assertion by demonstrating the presence of PHF and straight filaments, the ultrastructural components of NFT (Kosik et al. 1988; Lee et al. 2001), both of which have a size and periodicity within the ranges observed in human disease (Crowther 1991; Crowther et al., 1992).

Pathological tau hyperphosphorylation and NFT formation have also been observed in mice overexpressing the FTDP-17-causing P301L mutation (Lewis et al. 2000). However, it remains controversial whether this phosphorylation is a primary event or a secondary consequence of altered tau conformation in AD and other neurodegenerative conditions, despite evidence that phosphorylation directly precedes filament formation in vitro. GSK-3 $\beta$ , by virtue of its role as a major tau kinase (Lovestone et al., 1994; Sperber et al., 1995; Zheng-Fischhofer et al., 1998), its formation of a complex with tau in the microtubule fraction from bovine brain (Sun et al. 2002), and its colocalization with phosphorylated tau during development (Brion et al., 2001) is a leading candidate for initiating pathologic tau hyperphosphorylation. The data presented here demonstrate that hyper-

phosphorylation of tau by GSK-3 $\beta$  accelerates neurodegeneration and causes fibrillary tau-immunoreactive inclusions *in vivo*, confirming previous *in vitro* studies (Wille et al., 1992; Crowther et al., 1992; Lovestone et al., 1994; Sperber et al., 1995; Brion et al., 2001).

Enhancement of tau aggregation following GSK-3 $\beta$  phosphorylation was also observed in a mouse model of inducible GSK-3 $\beta$  overexpression in the presence of wild-type murine tau in which increased insoluble tau and pretangles were observed without NFT *per se* (Lucas et al., 2001). This observation agrees with data reported here, demonstrating that the combination of GSK-3 $\beta$  overexpression and wild-type tau dysregulation produces neurofibrillary pathology. Axonopathy, tau hyperphosphorylation, and pretangle formation have also been observed in mice overexpressing wild-type htau4R in the absence of GSK-3 $\beta$  activation, consistent with the mild tau phosphorylation observed in gl-tau flies. Surprisingly, constitutive GSK-3 $\beta$  activation and wild-type 4R tau phosphorylation actually ameliorated the pathology in another transgenic model (Spittaels et al., 2000). This finding contrasts with other *in vitro* and *in vivo* studies, including that reported here, which demonstrate enhancement of neurodegeneration coincident with tau hyperphosphorylation (Anderton et al., 2000; Lee et al., 2001). This apparent contradiction may be due to differences in promoters, expression levels, or genetic background effects.

It is unknown whether tau phosphorylation by kinases other than GSK-3 $\beta$  (e.g., Cdk5) has similar consequences to those observed here; the role of these and other factors (such as phosphatases) can now be investigated using this experimental paradigm. Nor is it known whether the amyloid-induced tau hyperphosphorylation and NFT formation observed recently in mutant tau transgenic mice (Gotz et al., 2001; Lewis et al., 2001) occurs via tau phosphorylation by GSK-3 $\beta$  or an alternate pathway. However, these data identify GSK-3 $\beta$  as a potential candidate for mediating amyloid-induced NFT formation in the presence of tau dysregulation.

#### The Role of NFT Formation in Neurodegeneration

Observations of neurodegenerative changes without NFT in humans harboring tau mutations (Houlden et al., 1999; Morris et al., 2001) and in transgenic *Drosophila* (Wittmann et al., 2001; the present study) call into question the causal role of tau aggregation and NFT formation in neurodegeneration. The circumstantial association of NFT with early morphological changes in neurons from postmortem human AD brains has long suggested a causal role for NFT formation in AD (Braak and Braak, 1994). While definitive answers are beyond the scope of any single investigation, our results, as well as those of Feany and colleagues (Wittmann et al., 2001), may provide some important clues.

We observed a correlation between the severity of neurodegeneration and the presence of insoluble hyperphosphorylated tau. Although Feany and coworkers (Wittmann et al., 2001) did not observe NFT in their model, the accumulation of nonfilamentous, abnormally phosphorylated tau was sometimes associated with vacuoles and degenerating cells. This observation, in conjunction with the retinal degeneration observed with tau expression alone, suggests that neurotoxicity is due

to abnormal phosphorylation of tau, rather than NFT, *per se*. Thus, the formation of NFT or other large visible tau aggregates may reflect a relatively late or severe stage in the neurodegenerative process. However, since NFT are a defining characteristic of several neurodegenerative disorders (including AD and PSP) and are a robust and scorable marker, neurofibrillary pathology (such as that described here) is likely to prove useful in screening for disease modifiers. It is unlikely that any single experimental model will faithfully recapitulate all pathologic features of complex neurodegenerative conditions in humans. Nonetheless, these findings, using a genetically pliable organism, provide impetus for extending and confirming our observations in mammalian systems.

#### Comparison to Previous Fly Models

The neurodegenerative phenotype observed in this study with wild-type tau overexpression appeared as severe as that seen previously with mutant tau overexpression (Wittmann et al., 2001). This may, in part, reflect differences in the promoter systems employed, resulting in tau misexpression in a more restricted subset of cells within the eye, as reported by Feany and coworkers (Wittmann et al., 2001). That neurodegeneration of roughly equivalent severity is observed with wild-type and mutant human tau overexpression in the *Drosophila* eye argues against the notion that neurodegeneration observed with mutant tau overexpression is a mutation-specific effect (Wittmann et al., 2001). Our data would predict that more widespread expression of wild-type tau under control of the GMR-GAL4 driver, as opposed to the *elav*-GAL4 driver, would produce rough eyes irrespective of whether the tau transgene is mutant or wild-type.

Recently, the sequence and expression pattern of the *Drosophila* homolog of tau have been reported (Heidary and Fortini, 2001). However, information as to effects of mutations in or overexpression of fly tau is not available. We have not observed crossreactivity of human tau antibodies with endogenous fly proteins, consistent with the findings of others (Wittmann et al., 2001). It is unknown whether interaction with endogenous fly tau plays a role in human tau-induced neurodegeneration and tau aggregation in our model, but this possibility can now be examined.

Neurodegenerative disease-causing mutations that are thought to induce a toxic gain-of-function are, in many respects, excellent candidates to be modeled in *Drosophila* (Fortini and Bonini, 2000; Jackson et al., 1998; Jackson 2000; Muqit and Feany, 2002). On the other hand, expression of nonmutant counterparts of disease-associated proteins may also provide important insights into neurodegenerative mechanisms. For example, pan-neural expression of wild-type  $\alpha$ -synuclein produces Lewy bodies and neurodegeneration (Feany and Bender, 2000). Both wild-type and mutant presenilins cause apoptosis in *Drosophila* (Fortini and Bonini, 2000). In this context, it is perhaps more useful to view *Drosophila* paradigms employing misexpression of disease-associated proteins as genetically sensitized systems for identifying candidate modifiers rather than strictly as models for dominantly acting gain-of-function disorders. Fly models, such as those reported here and else-

where, may yield important clues regarding disorders of tau dysregulation (including AD) in addition to the rarer cases of FTDP-17 cases caused by tau mutations.

#### Experimental Procedures

##### Genetics

A cDNA encoding wild-type htau4R was subcloned into the pExpress-*gl* modification (Ollmann et al., 2000) of the GMR expression vector (Hay et al., 1994). Embryos of the  $y^w^{1118}$  genotype were microinjected, and one transgenic line was obtained by standard methods (Rubin and Spradling, 1982; Spradling and Rubin, 1982); additional lines were derived by transposition from the original transformant. A total of five lines were obtained and two selected for use in these studies: line 1.1, which shows a severe phenotype, is on the second chromosome, and line 2.1, which shows a moderate phenotype, on the third. Standard genetic markers and chromosomes were used as described (Lindsley and Zimm, 1992). For immunofluorescence analysis in the adult, stocks were placed in a *cinnabar*, *brown* (*cn*, *bw*) homozygous background, which eliminates pigment formation and decreases autofluorescence. All crosses were carried out at 25°C. Adult flies were used for analysis 1–2 days posteclosion. The *elav*-GAL4<sup>c155</sup> (Lin and Goodman, 1994), *sev*-GAL4 (Brunner et al., 1994), *sevEP*-GAL4 (Therrien et al., 1999), *arm*<sup>1</sup> (Perrimon and Mahowald, 1987), *arm*<sup>4</sup> (Wieschaus and Rigglerman, 1987), *sgg*<sup>1</sup> (Judd et al., 1972), UAS-*arm*.S10 (Pai et al., 1997), dTCF<sup>2</sup>, and UAS-dTCF (van de Wetering et al., 1997) lines were obtained from the Bloomington Stock Center. The UAS-*arm*.S10 transgene expresses an Armadillo protein with a deletion of the Shaggy phosphorylation site, resulting in its stabilization. The UAS-*sgg* (Steitz et al., 1998) line was the kind gift of Dr. E. Siegfried. We refer to the *sev*-GAL4 line (Brunner et al., 1994), which uses the hsp70 promoter with the *sev* enhancer, as *sev*-GAL4 (S, for “strong”) and the *sevEP*-GAL4 (Therrien et al., 1999), which used a *sevenless*-derived (rather than a hsp70-derived) promoter, such as *sev*-GAL4 (W, for “weak”).

##### Histology and Immunohistochemistry

For SEM, flies were dehydrated in ethanol, incubated overnight in hexamethyldisilazane, dried under vacuum, attached to stubs with black nail polish, and analyzed using a Hitachi SEM. Plastic 2  $\mu$ m sections of adult retina were prepared and stained with toluidine blue, as described previously (Jackson et al., 1998). Cryostat sections (10  $\mu$ m) of adult heads were performed, as described previously (Jackson et al., 1998); primary antibodies were T14 (1  $\mu$ g/ml; Zymed) and AT100 (200 ng/ml; Pierce-Endogen) with Cy3-conjugated goat anti-mouse secondary (1:500; Jackson Labs). Stained sections were mounted in Vectashield with DAPI (Vector Labs) to counterstain nuclei. Samples were analyzed on a Biorad laser scanning confocal microscope. For the *gl*-tau lines, a low level of diffuse staining was seen in the absence of *shaggy* overexpression; for analysis of NFT formation, iris and gain were decreased to minimize staining in the absence of *shaggy* overexpression, but samples were analyzed under identical conditions. Z stacks (merged images) were constructed from ten focal planes for each final image. Staining of larval eye imaginal discs was performed, as described previously (Jackson et al., 1998). Antibodies used were rat monoclonal anti-Elav (1:100; O’Neill et al., 1994) and rabbit polyclonal anti-lamin (1:200; Smith and Fisher, 1989). Phalloidin-rhodamine (Sigma) and antibody staining of pupal eye discs were performed as previously described (Sang and Ready, 2002). AT100 staining in larvae and pupae used a concentration of 10  $\mu$ g/ml. For pupal and larval staining, secondary antibodies (Jackson Labs) were used at a 1:100 dilution.

##### Immunoblotting and Filament Preparation

Protein extraction was performed from three independent pools of 30 *Drosophila* heads for each condition and cortical tissue from postmortem AD brain. We prepared tissue lysates by well-characterized methods (Goedert et al., 1992). Determination of protein concentration was performed using the Bradford reagent (Biorad). Protein aliquots were resolved by 10% SDS-PAGE after adjustment of concentration, electrotransferred to PVDF membrane (Biorad), and

blotted with T14 or AT100. Immunoblots were developed with peroxidase-conjugated secondary antibody and enhanced chemiluminescence (Pierce) and quantified using a laser scanning densitometer (Molecular Dynamics). The remaining protein was used for extraction with N-lauroylsarcosinate and EM analysis using phosphotungstate negative staining similar to Goedert et al. (1992). Micrographs were recorded on a JEOL TEM at an operating voltage of 80 KV with a nominal magnification of 19,000 $\times$ .

##### Acknowledgments

We thank V.M.-Y. Lee for the htau4R cDNA; E. Siegfried, B. Hay, and the Bloomington Stock Center for fly strains; P. Fisher for the lamin antibody; Z. Luo for excellent technical support; and B. Sjöstrand for assistance with TEM. The *elav* monoclonal antibody was obtained from the Developmental Studies Hybridoma Bank developed under the auspices of NICHD and maintained by the University of Iowa. We also thank Larry Zipursky for critical comments on the manuscript and Dr. Robert Collins for his support of the Neurogenetics program. This work was supported by the NINDS (G.R.J.) the John Douglas French Alzheimer Foundation (D.H.G., M.W.-P.), the UCLA Neurogenetics program (G.R.J., D.H.G.), and the NIA-funded UCLA Alzheimer’s Disease Research Center (G.R.J., D.H.G.).

Received: March 29, 2002

Revised: April 23, 2002

##### References

- Ahmed, Y., Hayashi, S., Levine, A., and Wieschaus, E. (1998). Regulation of armadillo by a *Drosophila* APC inhibits neuronal apoptosis during retinal development. *Cell* 93, 1171–1182.
- Anderton, B.H., Dayanandan, R., Killick, R., and Lovestone, S. (2000). Does dysregulation of the Notch and wingless/Wnt pathways underlie the pathogenesis of Alzheimer’s disease? *Mol. Med. Today* 6, 54–59.
- Augustinack, J.C., Schneider, A., Mandelkow, E.M., and Hyman, B.T. (2002). Specific tau phosphorylation sites correlate with severity of neuronal cytopathology in Alzheimer’s disease. *Acta. Neuropathol.* 103, 26–35.
- Braak, H., and Braak, E. (1994). Morphological criteria for the recognition of Alzheimer’s disease and the distribution pattern of cortical changes related to this disorder. *Neurobiol. Aging* 15, 355–356.
- Brand, A.H., and Perrimon, N. (1993). Targeted gene expression as a means of altering cell fates and generating dominant phenotypes. *Development* 118, 401–415.
- Brion, J.P., Anderton, B.H., Authelat, M., Dayanandan, R., Leroy, K., Lovestone, S., Octave, J.N., Pradier, L., Touchet, N., and Tremp, G. (2001). Neurofibrillary tangles and tau phosphorylation. *Biochem. Soc. Symp.*, 81–88.
- Brunner, D., Ducker, K., Oellers, N., Hafen, E., Scholz, H., and Klambt, C. (1994). The ETS domain protein pointed-P2 is a target of MAP kinase in the sevenless signal transduction pathway. *Nature* 370, 386–389.
- Brunner, E., Peter, O., Schweizer, L., and Basler, K. (1997). Pangolin encodes a Lef-1 homologue that acts downstream of Armadillo to transduce the Wingless signal in *Drosophila*. *Nature* 385, 829–833.
- Cadigan, K.M., and Nusse, R. (1997). Wnt signaling: a common theme in animal development. *Genes Dev.* 11, 3286–3305.
- Clark, L.N., Poorkaj, P., Wszolek, Z., Geschwind, D.H., Nasreddine, Z.S., Miller, B., Li, D., Payami, H., Awert, F., Markopoulou, K., et al. (1998). Pathogenic implications of mutations in the tau gene in pallido-ponto-nigral degeneration and related neurodegenerative disorders linked to chromosome 17. *Proc. Natl. Acad. Sci. USA* 95, 13103–13107.
- Crowther, R.A. (1991). Straight and paired helical filaments in Alzheimer’s disease have a common structural unit. *Proc. Natl. Acad. Sci. USA* 88, 2288–2292.
- Crowther, R.A., Olesen, O.F., Jakes, R., and Goedert, M. (1992). The microtubule binding repeats of tau protein assemble into filaments like those found in Alzheimer’s disease. *FEBS Lett.* 309, 199–202.

- Dale, T.C. (1998). Signal transduction by the Wnt family of ligands. *Biochem. J.* 329, 209–223.
- Elyaman, W., Terro, F., Wong, N.S., and Hugon, J. (2002). In vivo activation and nuclear translocation of phosphorylated glycogen synthase kinase-3 $\beta$  in neuronal apoptosis: links to tau phosphorylation. *Eur. J. Neurosci.* 15, 651–660.
- Fan, S.S., and Ready, D.F. (1997). Glued participates in distinct microtubule-based activities in *Drosophila* eye development. *Development* 124, 1497–1507.
- Feany, M.B., and Bender, W.W. (2000). A *Drosophila* model of Parkinson's disease. *Nature* 404, 394–398.
- Fortini, M.E., and Bonini, N.M. (2000). Modeling human neurodegenerative diseases in *Drosophila*: on a wing and a prayer. *Trends Genet.* 16, 161–167.
- Freeman, M., and Bienz, M. (2001). EGF receptor/Rolled MAP kinase signalling protects cells against activated Armadillo in the *Drosophila* eye. *EMBO Rep.* 2, 157–162.
- Furukawa, K., D'Souza, I., Crudder, C.H., Onodera, H., Itoyama, Y., Poorkaj, P., Bird, T.D., and Schellenberg, G.D. (2000). Pro-apoptotic effects of tau mutations in chromosome 17 frontotemporal dementia and parkinsonism. *Neuroreport* 11, 57–60.
- Geschwind, D.H., and Miller, B.L. (2001). Molecular approaches to cerebral laterality: development and neurodegeneration. *Am. J. Med. Genet.* 101, 370–381.
- Geschwind, D.H., Robidoux, J., Alarcon, M., Miller, B.L., Wilhelmsen, K.C., Cummings, J.L., and Nasreddine, Z.S. (2001). Dementia and neurodevelopmental predisposition: cognitive dysfunction in pre-symptomatic subjects precedes dementia by decades in frontotemporal dementia. *Ann. Neurol.* 50, 741–746.
- Godemann, R., Biernat, J., Mandelkow, E., and Mandelkow, E.M. (1999). Phosphorylation of tau protein by recombinant GSK-3 $\beta$ : pronounced phosphorylation at select Ser/Thr-Pro motifs but no phosphorylation at Ser262 in the repeat domain. *FEBS Lett.* 454, 157–164.
- Goedert, M., Spillantini, M.G., Cairns, N.J., and Crowther, R.A. (1992). Tau proteins of Alzheimer paired helical filaments: abnormal phosphorylation of all six brain isoforms. *Neuron* 8, 159–168.
- Goedert, M., Crowther, R.A., and Spillantini, M.G. (1998). Tau mutations cause frontotemporal dementias. *Neuron* 21, 955–958.
- Goedert, M., Ghetti, B., and Spillantini, M.G. (2000). Tau gene mutations in frontotemporal dementia and parkinsonism linked to chromosome 17 (FTDP-17). Their relevance for understanding the neurodegenerative process. *Ann. NY Acad. Sci.* 920, 74–83.
- Gotz, J., Chen, F., van Dorpe, J., and Nitsch, R.M. (2001). Formation of neurofibrillary tangles in P301L tau transgenic mice induced by A $\beta$  42 fibrils. *Science* 293, 1491–1495.
- Greaves, S., Sanson, B., White, P., and Vincent, J.P. (1999). A screen for identifying genes interacting with armadillo, the *Drosophila* homolog of beta-catenin. *Genetics* 153, 1753–1766.
- Hanger, D.P., Hughes, K., Woodgett, J.R., Brion, J.P., and Anderton, B.H. (1992). Glycogen synthase kinase-3 induces Alzheimer's disease-like phosphorylation of tau: generation of paired helical filament epitopes and neuronal localisation of the kinase. *Neurosci. Lett.* 147, 58–62.
- Hasegawa, S., Sato, T., Akazawa, H., Okada, H., Maeno, A., Ito, M., Sugitani, Y., Shibata, H., Miyazaki, J., Katsuki, M., et al. (2002). Apoptosis in neural crest cells by functional loss of APC tumor suppressor gene. *Proc. Natl. Acad. Sci. USA* 99, 297–302.
- Hay, B.A., Wolff, T., and Rubin, G.M. (1994). Expression of baculovirus P35 prevents cell death in *Drosophila*. *Development* 120, 2121–2129.
- Hay, B.A., Wassarman, D.A., and Rubin, G.M. (1995). *Drosophila* homologs of baculovirus inhibitor of apoptosis proteins function to block cell death. *Cell* 83, 1253–1262.
- Heidary, G., and Fortini, M.E. (2001). Identification and characterization of the *Drosophila* tau homolog. *Mech. Dev.* 108, 171–178.
- Hetman, M., Cavanaugh, J.E., Kimelman, D., and Xia, Z. (2000). Role of glycogen synthase kinase-3 $\beta$  in neuronal apoptosis induced by trophic withdrawal. *J. Neurosci.* 20, 2567–2574.
- Hoffmann, R., Lee, V.M.-Y., Leight, S., Varga, I., and Otvos, L., Jr. (1997). Unique Alzheimer's disease paired helical filament specific epitopes involve double phosphorylation at specific sites. *Biochemistry* 36, 8114–8124.
- Hong, M., Zhukareva, V., Vogelsberg-Ragaglia, V., Wszolek, Z., Reed, L., Miller, B.L., Geschwind, D.H., Bird, T.D., McKeel, D., Goate, A., et al. (1998). Mutation-specific functional impairments in distinct tau isoforms of hereditary FTDP-17. *Science* 282, 1914–1917.
- Houlden, H., Baker, M., Adamson, J., Grover, A., Waring, S., Dickson, D., Lynch, T., Boeve, B., Petersen, R.C., Pickering-Brown, S., et al. (1999). Frequency of tau mutations in three series of non-Alzheimer's degenerative dementia. *Ann. Neurol.* 46, 243–248.
- Hutton, M., Lendon, C.L., Rizzu, P., Baker, M., Froelich, S., Houlden, H., Pickering-Brown, S., Chakraverty, S., Isaacs, A., Grover, A., et al. (1998). Association of missense and 5'-splice-site mutations in tau with the inherited dementia FTDP-17. *Nature* 393, 702–705.
- Ishiguro, K., Shiratsuchi, A., Sato, S., Omori, A., Arioka, M., Kobayashi, S., Uchida, T., and Imahori, K. (1993). Glycogen synthase kinase 3 $\beta$  is identical to tau protein kinase I generating several epitopes of paired helical filaments. *FEBS Lett.* 325, 167–172.
- Jackson, G.R. (2000). Modeling neurodegenerative diseases in the fruit fly. In *Molecular Mechanisms of Neurodegenerative Diseases*, M.F. Chesselet, ed. (Totowa, New Jersey: Human Press), pp. 373–406.
- Jackson, G.R., Salecker, I., Dong, X., Yao, X., Arnheim, N., Faber, P.W., MacDonald, M.E., and Zipursky, S.L. (1998). Polyglutamine-expanded human huntingtin transgenes induce degeneration of *Drosophila* photoreceptor neurons. *Neuron* 21, 633–642.
- Judd, B.H., Shen, M.W., and Kaufman, T.C. (1972). The anatomy and function of a segment of the X chromosome of *Drosophila melanogaster*. *Genetics* 71, 139–156.
- Killick, R., Pollard, C.C., Asuni, A.A., Mudher, A.K., Richardson, J.C., Rupniak, H.T., Sheppard, P.W., Varndell, I.M., Brion, J.P., Levey, A.I., et al. (2001). Presenilin 1 independently regulates beta-catenin stability and transcriptional activity. *J. Biol. Chem.* 276, 48554–48561.
- Kirschenbaum, F., Hsu, S.C., Cordell, B., and McCarthy, J.V. (2001). Glycogen synthase kinase-3 $\beta$  regulates presenilin 1 C-terminal fragment levels. *J. Biol. Chem.* 276, 30701–30707.
- Kosik, K.S., Orecchio, L.D., Binder, L., Trojanowski, J.Q., Lee, V.M., and Lee, G. (1988). Epitopes that span the tau molecule are shared with paired helical filaments. *Neuron* 1, 817–825.
- Lazebnik, Y.A., Takahashi, A., Moir, R.D., Goldman, R.D., Poirier, G.G., Kaufmann, S.H., and Earnshaw, W.C. (1995). Studies of the lamin proteinase reveal multiple parallel biochemical pathways during apoptotic execution. *Proc. Natl. Acad. Sci. USA* 92, 9042–9046.
- Lee, V.M., Goedert, M., and Trojanowski, J.Q. (2001). Neurodegenerative tauopathies. *Annu. Rev. Neurosci.* 24, 1121–1159.
- Lewis, J., McGowan, E., Rockwood, J., Melrose, H., Nacharaju, P., Van Slegtenhorst, M., Gwinn-Hardy, K., Paul Murphy, M., Baker, M., Yu, X., et al. (2000). Neurofibrillary tangles, amyotrophy and progressive motor disturbance in mice expressing mutant (P301L) tau protein. *Nat. Genet.* 25, 402–405.
- Lewis, J., Dickson, D.W., Lin, W.L., Chisholm, L., Corral, A., Jones, G., Yen, S.H., Sahara, N., Skipper, L., Yager, D., et al. (2001). Enhanced neurofibrillary degeneration in transgenic mice expressing mutant tau and APP. *Science* 293, 1487–1491.
- Lin, D.M., and Goodman, C.S. (1994). Ectopic and increased expression of Fasciclin II alters motoneuron growth cone guidance. *Neuron* 13, 507–523.
- Lindsley, D., and Zimm, G.G. (1992). *The Genome of Drosophila melanogaster* (San Diego: Academic Press).
- Liu, C., Li, Y., Semenov, M., Han, C., Baeg, G.-H., Tan, Y., Zhang, Z., Lin, X., and He, X. (2002). Control of beta-catenin phosphorylation/degradation by a dual kinase mechanism. *Cell* 108, 837–847.
- Lovestone, S., Reynolds, C.H., Latimer, D., Davis, D.R., Anderton, B.H., Gallo, J.M., Hanger, D., Mulot, S., Marquardt, B., Stabel, S., et al. (1994). Alzheimer's disease-like phosphorylation of the microtubule-associated protein tau by glycogen synthase kinase-3 in transfected mammalian cells. *Curr. Biol.* 4, 1077–1086.

- Lucas, J.J., Hernandez, F., Gomez-Ramos, P., Moran, M.A., Hen, R., and Avila, J. (2001). Decreased nuclear beta-catenin, tau hyperphosphorylation and neurodegeneration in GSK-3beta conditional transgenic mice. *EMBO J.* 20, 27–39.
- Ma, C., and Moses, K. (1995). Wingless and patched are negative regulators of the morphogenetic furrow and can affect tissue polarity in the developing *Drosophila* compound eye. *Development* 121, 2279–2289.
- Mandelkow, E.M., Drewes, G., Biernat, J., Gustke, N., Van Lint, J., Vandenheede, J.R., and Mandelkow, E. (1992). Glycogen synthase kinase-3 and the Alzheimer-like state of microtubule-associated protein tau. *FEBS Lett.* 314, 315–321.
- Matsuo, E.S., Shin, R.W., Billingsley, M.L., Van deVoorde, A., O'Connor, M., Trojanowski, J.Q., and Lee, V.M. (1994). Biopsy-derived adult human brain tau is phosphorylated at many of the same sites as Alzheimer's disease paired helical filament tau. *Neuron* 13, 989–1002.
- McCall, K., and Steller, H. (1998). Requirement for DCP-1 caspase during *Drosophila* oogenesis. *Science* 279, 230–234.
- Morris, H.R., Khan, M.N., Janssen, J.C., Brown, J.M., Perez-Tur, J., Baker, M., Ozansoy, M., Hardy, J., Hutton, M., Wood, N.W., et al. (2001). The genetic and pathological classification of familial frontotemporal dementia. *Arch. Neurol.* 58, 1813–1816.
- Mudher, A., Chapman, S., Richardson, J., Asuni, A., Gibb, G., Pollard, C., Killick, R., Iqbal, T., Raymond, L., Varndell, I., et al. (2001). Dishevelled regulates the metabolism of amyloid precursor protein via protein kinase C/mitogen-activated protein kinase and c-Jun terminal kinase. *J. Neurosci.* 21, 4987–4995.
- Mulot, S.F., Hughes, K., Woodgett, J.R., Anderton, B.H., and Hanger, D.P. (1994). PHF-tau from Alzheimer's brain comprises four species on SDS-PAGE which can be mimicked by in vitro phosphorylation of human brain tau by glycogen synthase kinase-3 beta. *FEBS Lett.* 349, 359–364.
- Muqit, M.M.K., and Feany, M.F. (2002). Modelling neurodegenerative diseases in *Drosophila*: a fruitful approach? *Nat. Rev. Neurosci.* 3, 237–243.
- Oberhammer, F.A., Hochegger, K., Froschl, G., Tiefenbacher, R., and Pavelka, M. (1994). Chromatin condensation during apoptosis is accompanied by degradation of lamin A+B, without enhanced activation of cdc2 kinase. *J. Cell Biol.* 126, 827–837.
- Ollmann, M., Young, L.M., Di Como, C.J., Karim, F., Belvin, M., Robertson, S., Whittaker, K., Demsky, M., Fisher, W.W., Buchman, A., et al. (2000). *Drosophila* p53 is a structural and functional homolog of the tumor suppressor p53. *Cell* 101, 91–101.
- O'Neill, E.M., Rebay, I., Tjian, R., and Rubin, G.M. (1994). The activities of two Ets-related transcription factors required for *Drosophila* eye development are modulated by the Ras/MAPK pathway. *Cell* 78, 137–147.
- Pai, L.M., Orsulic, S., Bejsovec, A., and Peifer, M. (1997). Negative regulation of Armadillo, a Wingless effector in *Drosophila*. *Development* 124, 2255–2266.
- Palacino, J.J., Murphy, M.P., Murayama, O., Iwasaki, K., Fujiwara, M., Takashima, A., Golde, T.E., and Wolozin, B. (2001). Presenilin 1 regulates beta-catenin-mediated transcription in a glycogen synthase kinase-3-independent fashion. *J. Biol. Chem.* 276, 38563–38569.
- Peifer, M., and Polakis, P. (2000). Wnt signaling in oncogenesis and embryogenesis—a look outside the nucleus. *Science* 287, 1606–1609.
- Perrimon, N., and Mahowald, A.P. (1987). Multiple functions of segment polarity genes in *Drosophila*. *Dev. Biol.* 119, 587–600.
- Riggelman, B., Wieschaus, E., and Schedl, P. (1989). Molecular analysis of the armadillo locus: uniformly distributed transcripts and a protein with novel internal repeats are associated with a *Drosophila* segment polarity gene. *Genes Dev.* 3, 96–113.
- Robinow, S., and White, K. (1988). The locus *elav* of *Drosophila melanogaster* is expressed in neurons at all developmental stages. *Dev. Biol.* 126, 294–303.
- Rubin, G.M., and Spradling, A.C. (1982). Genetic transformation of *Drosophila* with transposable element vectors. *Science* 218, 348–353.
- Sang, T.K., and Ready, D.F. (2002). Eyes closed, a *Drosophila* p47 homolog, is essential for photoreceptor morphogenesis. *Development* 129, 143–154.
- Sanson, B., White, P., and Vincent, J.P. (1996). Uncoupling cadherin-based adhesion from wingless signalling in *Drosophila*. *Nature* 383, 627–630.
- Smith, D.E., and Fisher, P.A. (1989). Interconversion of *Drosophila* nuclear lamin isoforms during oogenesis, early embryogenesis, and upon entry of cultured cells into mitosis. *J. Cell Biol.* 108, 255–265.
- Smith, D.E., Gruenbaum, Y., Berrios, M., and Fisher, P.A. (1987). Biosynthesis and interconversion of *Drosophila* nuclear lamin isoforms during normal growth and in response to heat shock. *J. Cell Biol.* 105, 771–790.
- Sperber, B.R., Leight, S., Goedert, M., and Lee, V.M. (1995). Glycogen synthase kinase-3 beta phosphorylates tau protein at multiple sites in intact cells. *Neurosci. Lett.* 197, 149–153.
- Spittaels, K., Van den Haute, C., Van Dorpe, J., Geerts, H., Mercken, M., Bruynseels, K., Lasrado, R., Vandezande, K., Laenen, I., Boon, T., et al. (2000). Glycogen synthase kinase-3beta phosphorylates protein tau and rescues the axonopathy in the central nervous system of human four-repeat tau transgenic mice. *J. Biol. Chem.* 275, 41340–41349.
- Spradling, A.C., and Rubin, G.M. (1982). Transposition of cloned P elements into *Drosophila* germ line chromosomes. *Science* 218, 341–347.
- Steitz, M.C., Wickenheisser, J.K., and Siegfried, E. (1998). Overexpression of zeste white 3 blocks wingless signaling in the *Drosophila* embryonic midgut. *Dev. Biol.* 197, 218–233.
- Su, J.H., Nichol, K.E., Sitch, T., Sheu, P., Chubb, C., Miller, B.L., Tomaselli, K.J., Kim, R.C., and Cotman, C.W. (2000). DNA damage and activated caspase-3 expression in neurons and astrocytes: evidence for apoptosis in frontotemporal dementia. *Exp. Neurol.* 163, 9–19.
- Sun, W., Qureshi, H.Y., Cafferty, P.W., Sobue, K., Agarwal-Mawal, A., Neufeld, K.D., and Paudel, H.K. (2002). Glycogen synthase kinase-3 $\beta$  is complexed with tau protein in brain microtubules. *J. Biol. Chem.* 277, 11933–11940.
- Therrien, M., Wong, A.M., Kwan, E., and Rubin, G.M. (1999). Functional analysis of CNK in RAS signaling. *Proc. Natl. Acad. Sci. USA* 96, 13259–13263.
- van de Wetering, M., Cavallo, R., Dooijes, D., van Beest, M., van Es, J., Loureiro, J., Ypma, A., Hursh, D., Jones, T., Bejsovec, A., et al. (1997). Armadillo coactivates transcription driven by the product of the *Drosophila* segment polarity gene dTCF. *Cell* 88, 789–799.
- Wieschaus, E., and Riggelman, R. (1987). Autonomous requirements for the segment polarity gene armadillo during *Drosophila* embryogenesis. *Cell* 49, 177–184.
- Wille, H., Drewes, G., Biernat, J., Mandelkow, E.M., and Mandelkow, E. (1992). Alzheimer-like paired helical filaments and antiparallel dimers formed from microtubule-associated protein tau in vitro. *J. Cell Biol.* 118, 573–584.
- Willert, K., and Nusse, R. (1998). Beta-catenin: a key mediator of Wnt signaling. *Curr. Opin. Genet. Dev.* 8, 95–102.
- Williams, D.W., Tyrer, M., and Shepherd, D. (2000). Tau and tau reporters disrupt central projections of sensory neurons in *Drosophila*. *J. Comp. Neurol.* 428, 630–640.
- Wittmann, C.W., Wszolek, M.F., Shulman, J.M., Salvaterra, P.M., Lewis, J., Hutton, M., and Feany, M.B. (2001). Tauopathy in *Drosophila*: neurodegeneration without neurofibrillary tangles. *Science* 293, 711–714.
- Zheng-Fischhofer, Q., Biernat, J., Mandelkow, E.M., Illenberger, S., Godemann, R., and Mandelkow, E. (1998). Sequential phosphorylation of Tau by glycogen synthase kinase-3beta and protein kinase A at Thr212 and Ser214 generates the Alzheimer-specific epitope of antibody AT100 and requires a paired-helical-filament-like conformation. *Eur. J. Biochem.* 252, 542–552.